

## Nonminimal Lorentz Violation in Linearized Gravity

Matthew Mewes

*Physics Department, California Polytechnic State University  
San Luis Obispo, CA 93407, USA*

This contribution to the CPT'19 meeting provides a brief overview of recent theoretical studies of nonminimal Lorentz violation in linearized gravity. Signatures in gravitational waves from coalescing compact binaries are discussed.

The Standard-Model Extension (SME) is a general framework for studies of arbitrary realistic violations of Lorentz and CPT invariance. The SME has provided a theoretical base for hundreds of searches for Lorentz and CPT violations in particles and in gravity.<sup>1</sup> The leading-order violations in the particle sectors of the SME were written down more than two decades ago,<sup>2</sup> followed by the leading-order violations in gravity.<sup>3</sup> These violations modify the Standard Model of particle physics and General Relativity. Together they give the so-called minimal Standard-Model Extension (mSME).

A Lorentz-violating term in the SME action takes the form of a conventional tensor operator contracted with a tensor coefficient for Lorentz violation:

$$\delta S = \int d^4x \text{ (coefficient tensor)} \cdot \text{ (tensor operator)} . \quad (1)$$

The tensor coefficients for Lorentz violation act as Lorentz-violating background fields. Each violation can be classified according to the mass dimension  $d$  of the conventional operator in natural units with  $\hbar = c = 1$ . The mSME contains the violations of renormalizable dimensions  $d = 3, 4$ . Nonminimal violations are those with  $d \geq 5$ . Nonminimal extensions have been constructed for a number of sectors of the SME, including gauge-invariant electromagnetism,<sup>4</sup> neutrinos,<sup>5</sup> free Dirac fermions,<sup>6</sup> quantum electrodynamics,<sup>7</sup> General relativity,<sup>8,9</sup> and linearized gravity.<sup>9–14</sup>

The extension for linearized gravity includes all possible modifications to the usual linearized Einstein-Hilbert action that are quadratic in the metric fluctuation  $h_{\mu\nu} = g_{\mu\nu} - \eta_{\mu\nu}$ . Each unconventional term takes the

2

 form<sup>12</sup>

$$\delta S = \int d^4x \frac{1}{4} \mathcal{K}^{(d)\mu\nu\rho\sigma\alpha_1\dots\alpha_{d-2}} h_{\mu\nu} \partial_{\alpha_1} \dots \partial_{\alpha_{d-2}} h_{\rho\sigma} , \quad (2)$$

where  $\mathcal{K}^{(d)\mu\nu\rho\sigma\alpha_1\dots\alpha_{d-2}}$  are the coefficients for Lorentz violation. The coefficient tensors can be split into irreducible pieces with unique symmetries, giving fourteen different classes of Lorentz violation.<sup>13</sup> Three of these classes yield modifications that are invariant under the usual gauge transformation  $h_{\mu\nu} \rightarrow h_{\mu\nu} + \partial_{(\mu}\xi_{\nu)}$ . Restricting attention to the gauge-invariant violations, the Lorentz-violating parts can be written as<sup>12</sup>

$$S_{LV} = \int d^4x \frac{1}{4} h_{\mu\nu} (\hat{s}^{\mu\rho\nu\sigma} + \hat{q}^{\mu\rho\nu\sigma} + \hat{k}^{\mu\nu\rho\sigma}) h_{\rho\sigma} , \quad (3)$$

where the three operators

$$\begin{aligned} \hat{s}^{\mu\rho\nu\sigma} &= \sum s^{(d)\mu\rho\alpha_1\nu\sigma\alpha_2\dots\alpha_{d-2}} \partial_{\alpha_1} \dots \partial_{\alpha_{d-2}} , \\ \hat{q}^{\mu\rho\nu\sigma} &= \sum q^{(d)\mu\rho\alpha_1\nu\alpha_2\sigma\alpha_3\dots\alpha_{d-2}} \partial_{\alpha_1} \dots \partial_{\alpha_{d-2}} , \\ \hat{k}^{\mu\nu\rho\sigma} &= \sum k^{(d)\mu\alpha_1\nu\alpha_2\rho\alpha_3\sigma\alpha_4\dots\alpha_{d-2}} \partial_{\alpha_1} \dots \partial_{\alpha_{d-2}} \end{aligned} \quad (4)$$

contain the three types of gauge-invariant violations. The  $s$ - and  $k$ -type violations are CPT even, while  $q$ -type violations break CPT invariance. The sums in Eq. (4) are over even  $d \geq 4$  for  $s$ -type violations, odd  $d \geq 5$  for  $q$ -type, and even  $d \geq 6$  for  $k$ -type.

The gauge invariant limit provides a simple framework for studies of Lorentz violation in gravity, including studies of short-range gravity,<sup>9,10</sup> gravitational Čerenkov radiation,<sup>11</sup> and gravitational waves.<sup>12–14</sup> For gravitational waves, the violations give a modified phase velocity of the form<sup>12</sup>

$$v = 1 - \varsigma^0 \pm \sqrt{|\varsigma_{(+4)}|^2 + |\varsigma_{(0)}|^2} . \quad (5)$$

The effects of Lorentz violation are controlled by the frequency- and direction-dependent functions

$$\begin{aligned} \varsigma^0 &= \sum_{djm} \omega^{d-4} {}_0Y_{jm}(-\hat{v}) k_{(I)jm}^{(d)} , \\ \varsigma_{(\pm 4)} &= \sum_{djm} \omega^{d-4} {}_{\pm 4}Y_{jm}(-\hat{v}) (k_{(E)jm}^{(d)} \pm ik_{(B)jm}^{(d)}) , \\ \varsigma_{(0)} &= \sum_{djm} \omega^{d-4} {}_0Y_{jm}(-\hat{v}) k_{(V)jm}^{(d)} , \end{aligned} \quad (6)$$

where  $\omega$  is the angular frequency. Spin-weighted spherical harmonics  ${}_sY_{jm}$  are used to characterize the dependence on the direction of propagation

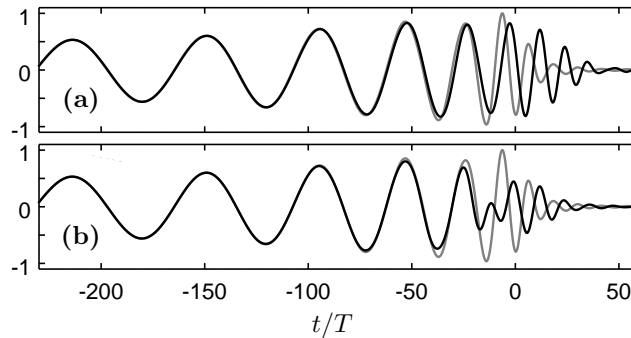


Fig. 1. Simulated noise-free detector strain signals from the merger of two equal-mass black holes for (a) nonbirefringent dispersion with  $\zeta^{(6)0} = 20T^3/\tau$  and (b) birefringence with  $\zeta_{(0)}^{(5)} = 10T^2/\tau$ . The effective propagation time  $\tau$  accounts for the redshift of the frequency during propagation. We also define the characteristic merger time scale  $T = G_N(1+z)M$  in terms of the Newton's constant  $G_N$  and the merger's redshift  $z$  and total mass  $M$ . The plots show the Lorentz-violating cases in black and the Lorentz-invariant limit in gray.<sup>14</sup>

$\hat{v}$ . The spherical coefficients for Lorentz violation  $k_{(I)jm}^{(d)}$ ,  $k_{(V)jm}^{(d)}$ ,  $k_{(E)jm}^{(d)}$  and  $k_{(B)jm}^{(d)}$  are complicated linear combinations of the underlying tensor coefficients in Eq. (4).

The Lorentz violation associated with  $k_{(I)jm}^{(d)}$  coefficients produce a frequency-dependent velocity, leading to direction-dependent dispersion in gravitational waves. An example of the effects of this type of violation in a binary merger is shown in the top plot of Fig. 1. In this example,  $d = 6$  violations lead to a shift in phase velocity that is proportional  $\omega^2$ . This particular shift causes the higher-frequency components of the wave to travel slower than lower-frequency parts. Early in the merger, when lower frequencies dominate, the effects of dispersion are insignificant. Higher frequencies dominate at later times, where the signal experiences a delayed arrival, deforming the tail end of the waveform.

The violations associated with the  $k_{(V)jm}^{(d)}$ ,  $k_{(E)jm}^{(d)}$  and  $k_{(B)jm}^{(d)}$  coefficients yield two distinct propagating solutions. The two solutions have different polarizations that are determined by the  $\zeta_{(+4)}$ ,  $\zeta_{(-4)}$ , and  $\zeta_{(0)}$  combinations.<sup>14</sup> Each solution propagates at a different speed, corresponding to the two signs in Eq. (5). This gives rise to birefringence (in addition to dispersion). A general wave is a superposition of the two solutions, which results in a net polarization that evolves as the wave propagates, yielding

a key signature of birefringence. The effects depend on frequency, so each frequency experiences a different change in polarization.

An example of the effects of birefringence are illustrated in the bottom plot of Fig. 1. In this example,  $d = 5$  birefringent Lorentz violations produce a simple rotation of the polarization of the wave. The rotation angle grows with  $\omega$ , so higher frequencies experience a greater change. The example assumes that the gravitational wave is linearly polarized and that the arms of the detector are aligned so that the strain signal is maximized in the Lorentz-invariant limit. At later stages in the merger, the higher frequencies produce a greater rotation of the polarization. This affects the relative alignment of the arms of the detector and the wave's polarization, decreasing the response of the detector and distorting the signal.

### Acknowledgments

This work was supported in part by the United States National Science Foundation under grant number 1819412.

### References

1. V.A. Kostelecký and N. Russell, *Data Tables for Lorentz and CPT Violation*, 2019 edition, arXiv:0801.0287v12.
2. V.A. Kostelecký and R. Potting, Phys. Rev. D **51**, 3923 (1995); D. Colladay and V.A. Kostelecký, Phys. Rev. D **55**, 6760 (1997); Phys. Rev. D **58**, 116002 (1998).
3. V.A. Kostelecký, Phys. Rev. D **69**, 105009 (2004); Q.G. Bailey and V.A. Kostelecký, Phys. Rev. D **74**, 045001 (2006); V.A. Kostelecký and J. Tasson, Phys. Rev. D **83**, 016013 (2011).
4. V.A. Kostelecký and M. Mewes, Phys. Rev. Lett. **99**, 011601 (2007); Ap. J. **689**, L1 (2008); Phys. Rev. D **80**, 015020 (2009); Phys. Rev. Lett. **110**, 201601 (2013).
5. V.A. Kostelecký and M. Mewes, Phys. Rev. D **85**, 096005 (2012).
6. V.A. Kostelecký and M. Mewes, Phys. Rev. D **88**, 096006 (2013).
7. Y. Ding and V.A. Kostelecký, Phys. Rev. D **94**, 056008 (2016); V.A. Kostelecký and Z. Li, Phys. Rev. D **99**, 056016 (2019).
8. Q.G. Bailey, Phys. Rev. D **94**, 065029 (2016).
9. Q.G. Bailey, V.A. Kostelecký, and R. Xu, Phys. Rev. D **91**, 022006 (2015).
10. V.A. Kostelecký and M. Mewes, Phys. Lett. B **766**, 137 (2017).
11. V.A. Kostelecký and J.D. Tasson, Phys. Lett. B **749**, 551 (2015).
12. V.A. Kostelecký and M. Mewes, Phys. Lett. B **757**, 510 (2016).
13. V.A. Kostelecký and M. Mewes, Phys. Lett. B **779**, 136 (2018).
14. M. Mewes, Phys. Rev. D **99**, 104062 (2019).